This is the accepted manuscript made available via CHORUS. The article has been published as:

Multipolar multiferroics in math xmlns="http://www.w3.org/1998/Math/MathML">mrow>mn>4/mn>msup>mi>d/mi>mn>2/mn>/msup>mo>//mo>mn>5/mn>msup>mi>d/mi>mn>2/mn>/msup>/mrow>/math> Mott insulators

Saikat Banerjee, Stephan Humeniuk, Alan R. Bishop, Avadh Saxena, and Alexander V. Balatsky

Phys. Rev. B **111**, L201107 — Published 12 May 2025

DOI: 10.1103/PhysRevB.111.L201107

Multipolar multiferroics in $4d^2/5d^2$ Mott insulators

Saikat Banerjee [1,2,*] Stephan Humeniuk [2] Alan R. Bishop,[1] Avadh Saxena [1] and Alexander V. Balatsky [3,4]

[1] *Theoretical Division, Los Alamos National Laboratory, Los Alamos, New Mexico 87545, USA*
[2] *Center for Materials Theory, Rutgers University, Piscataway, New Jersey, 08854, USA*
[3] *Nordita, KTH Royal Institute of Technology and Stockholm University, 106 91 Stockholm, Sweden*
[4] *Department of Physics, University of Connecticut, Storrs, Connecticut 06269, USA*

(Dated: May 2, 2025)

We extend the concept of conventional multiferroicity – where ferroelectric and ferromagnetic orders coexist – to include multipolar degrees of freedom. Specifically, we explore how this phenomenon emerges in $4d^2/5d^2$ Mott insulators with strong spin-orbit and Hund's couplings. Our study uncovers the origin of magnetic multipolar interactions in these systems and demonstrates that a combination of quadrupolar and octupolar magnetic order can simultaneously induce both electrical quadrupolar moments and ferroelectric polarization. By expanding the multiferroic framework to higher-order multipoles, we reveal the possibility of coexisting multipolar orders of different or same ranks, paving the way for new functional properties in a large class of strongly correlated materials.

Introduction.– Materials that exhibit coexisting magnetic and ferroelectric order, commonly known as multiferroics, open up a promising avenue for the mutual control of both magnetism and ferroelectricity. Although the research in multiferroics dates back to the 1950s [1], the recent advancements in theory, synthesis, and characterization techniques have significantly revived interest in these materials. Many candidate materials have been experimentally identified to harbor such coexisting dipolar orders [2, 3]. Notably, there is growing experimental evidence for materials exhibiting even multipolar (quadrupolar, octupolar, etc.) or the so-called hidden orders (HO) [4–7]. A compelling example is the long-standing puzzle of the HO phase transitions in URu_2Si_2 [8]. This intriguing phenomenon is linked to the presence of magnetic multipolar moments, which also interact with various electrical multipolar moments, rendering it a rich arena for exploration and understanding in condensed matter physics [9–15]. Therefore, it is natural to seek a microscopic description for coexisting multipolar orders.

Traditional multiferroic research [16–22] has mainly explored how dipolar limits of spin and charge degrees-of-freedom (DF) behave in different materials, including metals, semiconductors, and Mott insulators (MIs) [23–29]. In simple MIs, the electric charge is energetically gapped out, leaving only spins to determine the low-energy properties of the material. The arrangement of these spins creates various magnetic orders.

In certain MIs with strong spin-orbit coupling, a non-collinear spin pattern can break inversion symmetry, leading to ferroelectric polarization, known as the Katsura-Nagaosa-Balatsky (KNB) mechanism [7, 30–32]. Conversely, in some mixed-valence compounds (improper ferroelectrics), pre-existing ferroelectric polarization can generate magnetization [33, 34]. Interestingly, even magnetic systems that lack conventional order can still exhibit both magnetization and electric polarization, revealing new types of multiferroic behavior [35–37].

The complexity arises when a MI lacks any dipolar (spin) DF but is only governed by higher-order multipoles – a common scenario in heavy fermionic or $4d/5d$ transition metal (TM) compounds due to a subtle interplay of crystal field effects, Hund's coupling, and a large spin-orbit coupling (SOC) [38, 39]. Here dipolar order is absent; leading to first non-vanishing moment as quadrupole or octupole moment, etc. [40–46]. Although multipole contribution is typically weaker than the dipole order in common systems, its usefulness is of fundamental importance if the dipole component is intrinsically absent. This naturally leads to the question: can we expect an emergent ferroelectric polarization induced by such magnetic multipoles? More generally, is there a potential scheme for cross-coupling between the magnetic and electric multipoles?

Here, we demonstrate that d^2 ions with strong SOC and Hund's coupling can give rise to both ferroelectric polarization and electrical quadrupolar moments. We begin by examining the microscopic details of d^2 systems [41] and derive a multipolar exchange model relevant to edge-shared octahedral geometries. Using classical Monte Carlo (MC) simulations, we identify non-collinear magnetic octupolar textures (see Fig. 3), which suggest the possibility of induced ferroelectric response. Furthermore, our framework predicts a ferro-quadrupolar charge response that emerges purely from magnetic quadrupolar textures, even in the absence of non-collinearity – a key distinction from the conventional KNB-type multiferroicity.

The central result of our work is the framework for "multipolar multiferroicity", which extends the conventional multiferroic paradigm beyond dipole-dipole coupling. This insight opens up new avenues for exploring multipolar degrees of freedom and their novel functionalities in correlated materials. We also discuss potential experimental signatures and quantitative estimates

TABLE I. A summary of the higher-order multiferroic couplings. Notation: $l = 1 \rightarrow$ dipolar, $l = 2 \rightarrow$ quadrupolar, $l = 3 \rightarrow$ octupolar etc., and $l_{\mathrm{E(M)}} \rightarrow$ electrical (magnetic) sectors. The hetero-(homo)-geneous multiferroicity signifies coupling between different (same) order multipoles.

Conventional		Multipolar		
l_{E}	l_{M}	Type	l_{E}	l_{M}
-	-	Heterogeneous	1	3
1	1	Homogeneous	2	2
Ref. [26, 30]		This work		

to guide future studies.

Multipolar multiferroic framework.– Here, we present a simplified mathematical framework for the possible multipolar multiferroic coupling in MIs. We adopt a convention in which the "atomic" low-energy DF are characterized by the Stevens operators $\mathcal{O}_{lm}$ [47]. The lowest-order Stevens operators are simply the spin DF [39]. As we will see, in complex systems such as d^2 Mott insulators, the low-energy behavior is governed by higher-order Stevens operators, resulting in an effective multipolar exchange model. These higher-order interactions promote the emergence of diverse multipolar orders, including quadrupolar and octupolar states, in the parent Mott insulators [2, 41–45, 48].

Since the charge DF are gapped within a MI, the electric multipole moments can be induced only via the virtual exchange processes of the electrons with the ligand sites in the absence of doping. For a discrete charge distribution $\rho(\mathbf{r}_i)$, such multipole moments are defined as

$$\mathcal{Q}_{lm} = e\sum_{i=1}^{N}\int Z^*_{lm}(\hat{\delta\mathbf{r}}_i)\delta\mathbf{r}_i^l\psi^*_{\mathrm{f}}(\delta\mathbf{r}_i)\psi_{\mathrm{i}}(\delta\mathbf{r}_i)d^3\mathbf{r}, \quad (1)$$

where $Z_{lm}(\hat{\delta\mathbf{r}}_i) = \sqrt{\frac{4\pi}{2l+1}}Y_{lm}(\hat{\delta\mathbf{r}}_i)$ are the spherical harmonics with Racah normalization, $\delta\mathbf{r}_i = \mathbf{r} - \mathbf{r}_i$, N is the number of sites in a finite-size cluster, and $\psi_{\mathrm{f,i}}$ are the initial and final states during the virtual electron exchange processes. Subsequently, we adopt the real representation of $\mathcal{Q}_{lm}$ by constructing the tesseral harmonics as [47, 49]

$$\mathcal{Q}^{\mathrm{c}}_{lm} = (-1)^m\frac{\mathcal{Q}_{lm}+\mathcal{Q}^*_{lm}}{\sqrt{2}}, \quad \mathcal{Q}^{\mathrm{s}}_{lm} = (-1)^m\frac{\mathcal{Q}_{lm}-\mathcal{Q}^*_{lm}}{\sqrt{2}i}. \quad (2)$$

Rewriting Eq. (1) in this way is beneficial as both the electric and magnetic multipolar moments transform identically under the point-group representations of the underlying crystal. Under two discrete symmetries: parity/inversion ($\mathcal{P}$) and time-reversal ($\mathcal{T}$), the corresponding multipolar moments transform under these two symmetries as $\mathcal{P}: \mathcal{Q}^{\mathrm{c/s}}_{lm} \rightarrow (-1)^l\mathcal{Q}^{\mathrm{c/s}}_{lm}$, and $\mathcal{T}: \mathcal{O}_{lm} \rightarrow (-1)^l\mathcal{O}_{lm}$. Since they transform identically, the obvious possibility is whether a specific configuration of magnetic multipolar moments can trigger multipolar charge responses and vice versa. Our prediction of magnetic octupole-induced ferroelectricity and magnetic quadrupole-induced electrical quadrupolar responses exemplifies this concept and motivates us to propose an extended classification of multiferroics beyond conventional frameworks, as illustrated in Table I.

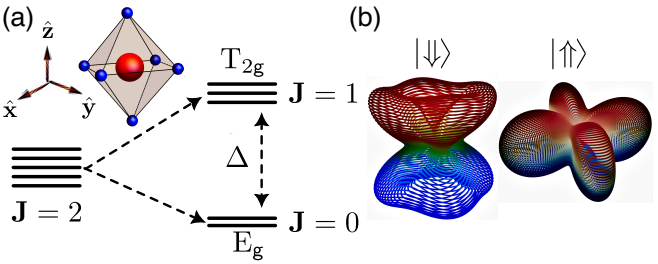


FIG. 1. (a) Left: Schematic of an octahedral unit-cell with TM atoms (red sphere) surrounded by the ligand (blue spheres). The crystal field further splits the $\mathbf{J} = 2$ states into a $\mathrm{E_g}$ doublet and a $\mathrm{T_{2g}}$ triplet. Right: The corresponding $\mathrm{T_{2g}}$, and $\mathrm{E_g}$ splitting of $\mathbf{J} = 2$ atomic energy levels under the influence of crystal field ($\Delta_{\mathrm{crys.}}$), Hund's coupling (J_{H}) and SOC (λ). Here, Δ denotes a renormalized crystal field acting on the $\mathbf{J} = 2$ manifold. (b) The spatial distribution of the charge density for the pseudo-spin up and down states.

Model.– We begin with a d^2 ion in an octahedral crystal field, where the atomic ground state is the non-Kramers $\mathrm{E_g}$ doublet characterized by the total angular momentum operator $\mathbf{J} = \mathbf{L}+\mathbf{S}$ [41]. The corresponding atomic energy splitting is illustrated in Fig. 1, with the $\mathrm{E_g}$ states given by

$$|\Uparrow\rangle = \frac{1}{\sqrt{2}}(|J_z = 2\rangle + |J_z = -2\rangle), \quad |\Downarrow\rangle = |J_z = 0\rangle\,. \quad (3)$$

The detailed spatial structure of these states with two spin-orbit coupled d-electrons in the crystal field splitting is given in the Supplementary Material (SM) [50]. The real-space charge distribution for the pseudo-spin states is shown in Fig. 1(b). We notice that the $|\Uparrow\rangle$-state is distributed along the xy-plane since one of the electrons has to occupy a d_{xy} orbital, while the $|\Downarrow\rangle$-state is elongated along the z-axis as two electrons can simultaneously occupy the d_{yz} and d_{zx} orbitals [50–57]. It is easy to show that the eigenstates in Eq. (3) host non-zero matrix elements between three higher-order magnetic Stevens operators, namely $\mathcal{O}_{20} = 3J_z^2 - \mathbf{J}^2$, $\mathcal{O}_{22} = J_x^2 - J_y^2$, and $\mathsf{T}_{xyz} = \overline{J_xJ_yJ_z}$ (average corresponds to symmetrization over all indices) [4, 40, 41, 43, 44]. Normalizing the operators as follows

$$\frac{\mathcal{O}_{22}}{4\sqrt{3}} \rightarrow \tilde{\sigma}^x, \qquad \frac{\mathsf{T}_{xyz}}{2\sqrt{3}} \rightarrow \tilde{\sigma}^y, \qquad \frac{\mathcal{O}_{20}}{12} \rightarrow \tilde{\sigma}^z, \quad (4)$$

it can be shown that they satisfy an effective SU(2) pseudo-spin algebra, *i.e.* $[\tilde{\sigma}^\alpha, \tilde{\sigma}^\beta] = i\epsilon_{\alpha\beta\gamma}\tilde{\sigma}^\gamma$.

At first, we note that under time-reversal symmetry (TRS) transformation, pseudo-spin operators transform as $\mathcal{T}: \{\tilde{\sigma}^x, \tilde{\sigma}^y, \tilde{\sigma}^z\} \rightarrow \{\tilde{\sigma}^x, -\tilde{\sigma}^y, \tilde{\sigma}^z\}$, as evident from

Eq. (4). This fact constrains the possible bilinear and trilinear exchange terms in the governing Hamiltonian. For example, terms including a single $\tilde{\sigma}^y$ like $\tilde{\sigma}_i^\eta \tilde{\sigma}_j^y (\eta = x, z)$ are not allowed in the bilinear exchange. Furthermore, the trilinear exchange may contain terms like $\tilde{\sigma}_i^y \tilde{\sigma}_j^y \tilde{\sigma}_k^{x/z}$ ($\forall\ i, j, k$ neighboring sites), and any other combinations. However, such terms would be forbidden by $\mathsf{C}_3^{[111]}$ symmetry, as $\tilde{\sigma}^x$, $\tilde{\sigma}^z$ transform like a conventional e_g orbital in a Kugel-Khomskii model [58–60], while $\tilde{\sigma}^y$ remains invariant. In general, the explicit form of the multipolar Hamiltonian can be complex, as it depends on the specific material properties. However, such an exchange Hamiltonian can, in principle, give rise to non-trivial multipolar textures, as we show below.

Ferroelectric polarization.– Without adhering to any specific scenario as mentioned earlier, here we take a local approximation of a generic multipolar Hamiltonian as $\mathcal{H}_{\rm local} = -\tilde{U} \sum_i \hat{\boldsymbol{e}}_i \cdot \tilde{\boldsymbol{\sigma}}_i$, where $\tilde{U}$ denotes the local excitation energy, and $\hat{\boldsymbol{e}}_i = (\cos\phi_i \sin\theta_i, \sin\phi_i \sin\theta_i, \cos\theta_i)$ describes the local orientation of the pseudo-spin moments at site i [30]. Next, for the virtual charge transfer process, we consider a four-site cluster of two TM and two ligand atoms in the edge-shared geometry as shown in Fig. 2(a). We focus on the stoichiometric configuration with electron *filled* ligand sites. Subsequently, we allow ligand-TM charge transfer processes in a double-exchange (DE) framework and consider two different hopping paths ($t_{pd}^\pi > 0$) in the upper and lower triangular plaquettes as in Fig. 2(a). The eigenstates are obtained by diagonalizing $\mathcal{H}_{\rm local}$ as follows

$$\begin{aligned} |\psi^+\rangle &= \cos\tfrac{\theta_i}{2} |\Uparrow\rangle + e^{i\phi_i} \sin\tfrac{\theta_i}{2} |\Downarrow\rangle, \\ |\psi^-\rangle &= \sin\tfrac{\theta_i}{2} |\Uparrow\rangle - e^{i\phi_i} \cos\tfrac{\theta_i}{2} |\Downarrow\rangle, \end{aligned} \tag{5}$$

where $|\Uparrow\rangle, |\Downarrow\rangle$ are the same as in Eq. (3), with energies $\mp\tilde{U}$. Assuming a finite TM-ligand hopping (t_{pd}^π), we compute the perturbation correction to the ground states in Eq. (5) leading to an intermediate configuration: d^3, p_z^1, where a strong Hund's coupling is considered for the d^3 ion in the octahedral crystal field. Utilizing these perturbed states $|\psi\rangle$ in the four-site cluster [50], we analyze the expectation value of the ferroelectric polarization $\mathbf{P} = \langle\psi|e\mathbf{r}|\psi\rangle$. We notice that for the z-bond, only x-component of $\mathbf{P}$ is finite and is given by

$$\langle P_x \rangle \approx \frac{e I t_{pd}^\pi}{3\Delta_{\rm crys.}} \cos\frac{\theta_i}{2} \cos\frac{\theta_j}{2} \sin(\phi_i - \phi_j), \tag{6}$$

where the overlap integral I is defined as $I \sim \int d\mathbf{r}\, x p_{\mathbf{r}}^z d_{\mathbf{r}}^{zx}$ and its cyclic permutations. The coordinate system is centered at the middle of the four-site cluster and aligned with the local octahedral coordinate axes. The emergent polarization is manifestly odd under inversion symmetry and is bond-dependent. For other bonds, the finite component is obtained by cyclic permutation of x, y, z. We note that without any octupolar component, *i.e.* $\phi_i = 0$, the polarization vanishes – aligning with our earlier phenomenological analysis (see Table I, heterogeneous type: $l_{\rm E} = 1, l_{\rm M} = 3$). Even a coplanar quadrupole order along with a non-collinear octupole part leads to a finite ferroelectric polarization. Unlike the KNB mechanism [30], this mechanism can generate a finite ferroelectric polarization without sharp features in neutron scattering, indicating absence of spin moments in materials with multipolar order. Approximating the orbitals by hydrogen-like wavefunctions, it is found that the overlap integral I is an order of magnitude larger for $4d$ and $5d$ orbitals compared to $3d$ orbitals. With typical lattice constants a rough estimate of the polarization is then $\langle P_x \rangle \sim (\frac{t_{pd}^\pi}{\Delta_{\rm crys.}}) \mu{\rm C\ cm}^{-2}$, similar to or even larger than the estimate in Ref. [30] for $3d$ orbitals.

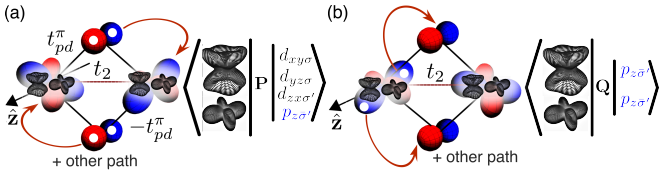


FIG. 2. The different hopping channels to the ligand p orbitals in a four-site cluster. (a) A double-exchange hopping from the ligand to the TM sites, and (b) a cotunneling of electrons (white filled circles) from the TM to the two ligand sites, relevant for ferroelectric polarization, and electrical quadrupolar moments, respectively. Other path corresponds to the remaining possible hopping in the left-over channel.

Electrical quadrupole moment.– We now turn to ferroquadrupolar charge distribution on the same geometry, however, focused on the stoichiometric configuration with electron *empty* ligand sites. A cotunneling process is considered, where each TM electron simultaneously hops to upper and lower empty ligand sites (such as boron group of elements), as illustrated in Fig. 2(b). This can be a weak but a physical process. We employ a similar perturbative approach and focus on the correction to the ground state in Eq. (5) leading to the intermediate configuration: d^0, p_z^1, p_z^1. Again utilizing the perturbed states $|\psi\rangle$ within the four-site cluster [50], we analyze the expectation value of the electrical multipole moment $\mathcal{Q}_{lm}$ as defined in Eq. (2). In this case, we find that for the z-bond only $\mathcal{Q}_{21}^{\rm s}$ and $\mathcal{Q}_{22}^{\rm s}$ are non-vanishing. Setting the origin at the center of the cluster, we obtain

$$\mathcal{Q}_{21}^{\rm s} \approx \frac{8eI'(t_{pd}^\pi)^2}{3\sqrt{3}\Delta_{\rm crys.}^2} \cos\frac{\theta_i}{2} \cos\frac{\theta_j}{2} \cos(\phi_i - \phi_j), \tag{7a}$$

$$\mathcal{Q}_{22}^{\rm s} \approx \frac{4eI'(t_{pd}^\pi)^2}{3\Delta_{\rm crys.}^2} \cos\frac{\theta_i}{2} \sin\frac{\theta_j}{2} \cos\phi_i + i \leftrightarrow j + \mathcal{Q}_{21}^{\rm s}, \tag{7b}$$

where the overlap integral is defined as $I' \sim \int d\mathbf{r} d_{\mathbf{r}}^{xy} d_{\mathbf{r}}^{zx} yz p_{\mathbf{r}}^z p_{\mathbf{r}}^z \approx I^2$, and its cyclic permutations. Here, l (l') corresponds to the upper (lower) ligand sites in Fig. 2(b). For other bonds, the non-vanishing

quadrupolar components are obtained by cyclic permutations of x, y, z. Note that, even without any magnetic octupolar moments, the electrical quadrupolar moment survives and arises only from the magnetic quadrupole, consistent with Table I, homogeneous type: $l_{\rm E} = 2, l_{\rm M} = 2$. To the best of our knowledge, this stands in sharp contrast to all known multiferroic mechanisms to date, and indeed provides a route to multipolar generalization. Taking a similar approach as before, the induced moment is estimated to be relatively small ($\sim 10^2(\frac{t^{\pi}_{pd}}{\Delta_{\rm crys.}})^2$ fC cm^{-1}) compared to the ferroelectric polarization.

Having obtained the multipolar response functions, we now explore the effective multipolar exchange interaction by performing perturbation theory on the Hubbard-Kanamori model. We consider an ideal edge-sharing octahedral geometry, and focus on the [111] plane, where the TM sites form a honeycomb lattice [41] (see inset in Fig. 3(b)). The microscopic Hamiltonian is given by $\mathcal{H} = \mathcal{H}_0 + \mathcal{H}_1$, where

$$\mathcal{H}_0 = U\sum_{i\alpha} n_{i\alpha\uparrow}n_{i\alpha\downarrow} + \frac{U'}{2}\sum_{\substack{i,\alpha\neq\beta\\ \sigma\sigma'}} n_{i\alpha\sigma}n_{i\beta\sigma'} + \Delta_{\rm crys.}\sum_{l,\sigma} n^p_{l\sigma} +$$

$$- \frac{J_{\rm H}}{2}\sum_{\substack{i,\alpha\neq\beta\\ \sigma\sigma'}} d^\dagger_{i\alpha\sigma}d_{i\alpha\sigma'}d^\dagger_{i\beta\sigma'}d_{i\beta\sigma} + \lambda\sum_{\substack{i,\alpha\beta\\ \sigma\sigma'}} d^\dagger_{i\alpha\sigma}\left(\mathbf{L}\cdot\mathbf{S}\right)^{\alpha\beta}_{\sigma\sigma'} d_{i\beta\sigma'},$$

$$\mathcal{H}_1 = \sum_{\substack{ij,\eta\\ \alpha\beta}} t^{(\eta)}_{\alpha\beta} d^\dagger_{i\alpha\sigma}d_{j\beta\sigma'} + t^{(\eta)}_{pd}\sum_{\substack{\langle il\rangle,\eta\\ \alpha\sigma}} p^\dagger_{l\sigma}d_{i\alpha\sigma} + \text{h.c.}, \qquad (8)$$

where U, U' denote the intra- and inter-orbital Coulomb repulsion, $J_{\rm H}$ is the Hund's coupling, $\Delta_{\rm crys.}$ denotes the ligand charge-transfer energy, and λ is the strength of the SOC, and $t^{(\eta)}_{\alpha\beta}, t'^{(\eta)}_{\alpha\beta}$ ($t^{(\eta)}_{pd}$) correspond to the various bond-dependent hopping amplitudes as shown in Fig. 2(b). For simplicity, we integrate out the ligand degrees of freedom and consider a renormalized TM-TM hopping as $t^{(\eta)}_{\alpha\beta} \to t^{(\eta)}_{\alpha\beta} + (t^{(\eta)}_{pd})^2/\Delta_{\rm crys.}$ [61], with $t^{(\eta)}_{\alpha\beta}$ obtained via Slater-Koster integrals [62]. Projecting Eq. (5) into the $\rm E_g$ doublet, we obtain the exchange Hamiltonian as $\mathcal{H} = \sum_\eta \mathcal{H}_\eta + \mathcal{H}^{(3)}$ where [50, 63, 64]

$$\mathcal{H}_\eta = J^{(2)}\sum_{\langle ij\rangle,\eta}\left(\tilde\sigma^y_i\tilde\sigma^y_j - \tilde\sigma^x_i\tilde\sigma^x_j - \tilde\sigma^z_i\tilde\sigma^z_j\right), \qquad (9)$$

and the bilinear exchange interaction is identical along all the bond directions $\eta \in \{x, y, z\}$ consistent with the cubic rotation symmetry of the pseudo-spin DF [41], and $J^{(2)} = 2t_2^2/(3\Delta E_{\rm ex.})$, where $\Delta E_{\rm ex.} = U - 3J_{\rm H} + \lambda$. The expression in Eq. (9) may give the misleading impression that the model remains valid even in the absence of $J_{\rm H}, \lambda$. However, it is true only in the presence of the non-Kramers doublet induced by Hund's coupling and SOC [see Fig. 1(a)]. This validity is further corroborated by numerical exact diagonalization calculations performed on a two-site cluster, as reported in Ref. [65]. The trilinear exchange term is inherently complex and becomes

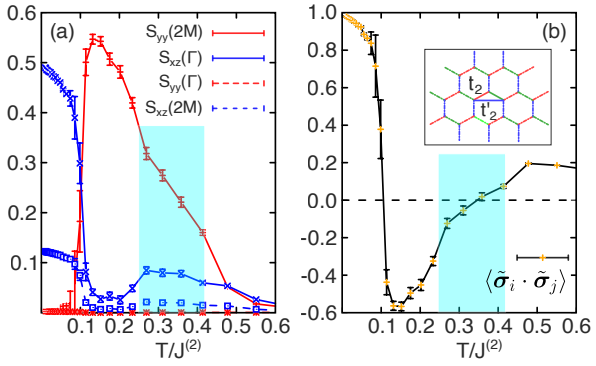


FIG. 3. (a) Structure factor of the octupolar (S_{yy}) and quadrupolar (S_{xz}) spin components at momentum points Γ and $2M$. The strength of the three-spin term is $\zeta = 0.15$ and the system size is $12 \times 12 \times 2$. For $T/J^{(2)} < 0.1$, the order is quadrupolar (xz) FM, whereas for $0.1 < T/J^{(2)} < 0.5$ it is octupolar (y) AFM. In the shaded region, the spin configuration is canted, i.e., (y) AFM and (xz) FM orders coexist. (b) Average scalar product between neighboring spins as a crude measure of collinearity. (Inset) A cartoon of the honeycomb structure with relevant hoppings as in Eq. (8). Different colors label different bond-types.

finite only when TRS is broken by an external field. Its explicit form is obtained through the third-order perturbation theory and, as discussed earlier, is constrained by both TRS and $\rm C_3$ symmetry. The latter reads as [50]

$$\mathcal{H}^{(3)} = \chi_s\sum_{\langle\!\langle ijk\rangle\!\rangle}\left(\alpha\tilde\sigma^x_i\tilde\sigma^x_j + \alpha\tilde\sigma^z_i\tilde\sigma^z_j - \beta\tilde\sigma^y_i\tilde\sigma^y_j\right)\tilde\sigma^y_k + P_{ijk}, \quad (10)$$

where $\langle\!\langle ijk\rangle\!\rangle$ denotes all possible triangles of nearest-neighbor sites on the honeycomb lattice, P_{ijk} indicates the cyclic permutations of the site indices i, j, k, $\chi_s = 2t_2^2t'_2/(3\Delta E^2_{\rm ex.})\sin\frac{e\Phi}{\hbar c}$, with Φ being the total flux in the triangular plaquette in an external magnetic field B [66], and $\alpha = \frac{2}{9}, \beta = \frac{1}{9}$ [50]. Here, we ignored the virtual hopping between $\rm T_{2g}$ and $\rm E_g$ sectors, and ignored the Zeeman coupling. However, we assumed the following hierarchy $U > \Delta_{\rm crys.} > J_{\rm H}, \lambda > B$ in the energy scales. The effect of a larger Zeeman coupling is known to induce quadrupole-octupole coupling as reported in a previous theoretical work [42].

Multipolar ordering.– Having derived the exchange Hamiltonian in Eqs. (9) and (10), we now utilize classical MC simulations to explore potential pseudo-spin textures in an external magnetic field, consistent with our local approximations used in the derivation of Eqs. (6), (7a), and (7b). In this regard, we tune the relative strength of the bilinear and trilinear terms in the Hamiltonian. We label this parameter as $\zeta = \chi_s/J^{(2)} = t'_2/\Delta E_{\rm ex.}\sin\frac{e\Phi}{\hbar c}$.

We adopt a classical approximation as $\tilde{\boldsymbol{\sigma}}_i = (\sin\theta_i\cos\phi_i, \sin\theta_i\sin\phi_i, \cos\theta_i)$, where each pseudo-spin is set to be an O(3) vector satisfying $|\tilde{\boldsymbol{\sigma}}_i\cdot\tilde{\boldsymbol{\sigma}}_i| = 1$. The simulations are performed using the standard Metropolis single-spin flip update [67] and parallel tempering [68]

with a geometric temperature grid. Without the three-spin term ($\zeta = 0$), the Hamiltonian in Eq. (9) can be recast as the Heisenberg antiferromagnet by a gauge transformation $\tilde{\sigma}_i^{x,z} \to -\tilde{\sigma}_i^{x,z}$ on one of the two sublattices, and the ground state is a Néel antiferromagnet. This corresponds to antiferromagnetically (AFM) aligned octupolar (y) components and ferromagnetically (FM) aligned quadrupolar (xz) components of equal strength.

As Fig. 3(a) shows, the three-spin term Eq. (10) changes the balance between octupolar and quadrupolar components: The ground state and low-temperature phase is xz FM, which is separated by a sharp spin-flop transition from a predominantly y AFM phase. This is evidenced by the static structure factor for the quadrupolar, $S_{xz}(\mathbf{q}) = \frac{1}{N^2}\sum_{ij} e^{i\mathbf{q}\cdot(\mathbf{r}_i-\mathbf{r}_j)}\langle \frac{1}{2}(\tilde{\sigma}_i^x\tilde{\sigma}_j^x + \tilde{\sigma}_i^z\tilde{\sigma}_j^z)\rangle$, and the octupolar, $S_{yy}(\mathbf{q}) = \frac{1}{N^2}\sum_{ij} e^{i\mathbf{q}\cdot(\mathbf{r}_i-\mathbf{r}_j)}\langle \tilde{\sigma}_i^y\tilde{\sigma}_j^y\rangle$ components: In the xz-FM phase $S_{xz}(\mathbf{q})$ has a peak at the center of the first Brillouin zone (BZ) $\Gamma = (0,0)$ and a second peak of 1/4 its strength at the point $2\mathrm{M} = (\frac{2\pi}{a}, \frac{2\pi}{\sqrt{3}a})$ at the center of the second BZ, which indicates intra-unit-cell order. Here, a is the lattice constant of the underlying triangular Bravais lattice as shown in Fig. 3(b). By contrast, in the y-AFM phase $S_y(2\mathrm{M})$ is large, while $S_{yy}(\Gamma)$ vanishes. Importantly, there is a finite-temperature window where both $S_{yy}(2\mathrm{M})$ and $S_{xz}(\Gamma)$ are non-zero and of unequal strength, which indicates a non-collinear, canted spin configuration that is AFM in y-components and FM in xz-components. This region is shaded in Fig. 3(a,b).

As a crude measure of collinearity we consider the scalar product between nearest neighbor pseudo-spins, $\langle \tilde{\boldsymbol{\sigma}}_i \cdot \tilde{\boldsymbol{\sigma}}_{\langle j\rangle_i}\rangle$, averaged over all bonds $(i, \langle j\rangle_i)$, which is shown in Fig. 3(b) and is consistent with a quadrupolar FM polarized state at low-temperatures and an octupolar AFM or canted state at intermediate temperatures. The implication of quantum or thermal fluctuations is an important question here but is beyond the scope of this work. This MC simulation for potential multipolar textures is an *ad hoc* and crude proof for the underlying approximations adopted earlier for the multiferroic responses in Eq. (6), and Eqs. (7a) and (7b).

Experimental signatures– Our proposed functionality can be realized in d^2/f^2 octahedral ions such as pressurized $ReCl_5$ [69], and WO_{3-x} [70] (relevant for ferroelectric polarization), or $[ReIn_6]^{3-}$, and $[Re(B_6H_6)]^{3-}$ [71] (relevant for ferroquadrupolar response) metal complexes. While detecting multipolar orders presents significant challenges, we outline several potential experimental probes. Magnetic octupolar order, for instance, can lead to transverse magnetic fields under shear strain – known as transverse piezomagnetism [72, 73]. Similarly, magnetic quadrupolar order can couple to specific normal modes of Jahn-Teller distortions [4, 41], which can be precisely measured using x-ray diffraction experiments, thereby indirectly confirming the magnetic quadrupolar orders [5]. Optical techniques such as second-harmonic generation or the Kerr effect can be employed to detect the presence of induced ferroelectric polarization. Although detecting ferroquadrupolar moments is exceptionally challenging, nuclear magnetic resonance spectroscopy may provide a viable pathway for its observation. Ab-initio [74], or cluster dynamical mean-field theory calculations [75], may provide more accurate and realistic estimates.

Discussion and perspective.– In this Letter, we proposed a mechanism generalizing the conventional multiferroicity to higher-order sectors. Even if the multipolar magnitudes are small compared to their dipolar counterparts, identifying materials where dipolar electric and magnetic moments vanish is fundamentally important, as it enables the exploration of novel coupled multipolar orders. Such materials can exhibit distinct phase transitions, topological excitations, and nonlinear responses, potentially leading to new functionalities in multiferroics and magnetoelectric applications. Specifically, we presented a scenario for cross-coupling between magnetic and electric quadrupole moments, as well as magnetic octupole moments, leading to ferroelectricity. This proposed mechanism can be readily extended to other spin-orbit coupled systems, including heavy-fermionic compound such as URu_2Si_2, and might be relevant to the puzzle of HO phase transitions. Our results lead to a refined classification of multiferroics, incorporating the multipolar sector, and opening new avenues for exploring the coupling of multipole moments beyond those listed in Table I.

Note added – A notable example is quadrupole-induced ferroelectricity, as discussed in a recent preprint [76], which aligns with and exemplifies the functionality we describe as "multipolar multiferroicity."

Acknowledgments.– We acknowledge helpful discussions with Gabriel Aeppli, Sang-Wook Cheong, Piers Coleman, Niels Grønbech-Jensen, Hosho Katsura, Giniyat Khaliullin, Naoto Nagaosa, and Wei Zhu. S.B. is grateful to the Department of Physics, University of Connecticut, Storrs, USA, for hosting, where part of the work was initiated. The work in Los Alamos was carried out under the auspices of the U.S. Department of Energy (DOE), Office of Science, and Office of Advanced Scientific Computing Research through the Quantum Internet to Accelerate Scientific Discovery Program. S.B. gratefully acknowledges partial support from the Office of Basic Energy Sciences, Material Sciences and Engineering Division, U.S. DOE, under Contract No. DE-FG02-99ER45790. Work of A.V.B was supported by U.S. Department of Energy, Office of Science, Office of Basic Energy Sciences under award number DE-SC- 0025580 and by European Research Council under the European Union Seventh Framework ERS-2018-SYG 810451 HERO. Computations were performed (S.H.) on the cluster of the Center for Materials Theory at the Department of Physics and Astronomy at Rutgers University.

Data availability.– The data that supports our findings in Fig. 3 is publicly available at Zenodo.

* saikat.banerjee@rutgers.edu

[1] L. D. Landau and E. M. Lifshitz, *Electrodynamics of Continuous Media* (Pergamon Press, 1984).

[2] Yao-Dong Li, Xiaoqun Wang, and Gang Chen, "Hidden multipolar orders of dipole-octupole doublets on a triangular lattice," Phys. Rev. B **94**, 201114(R) (2016).

[3] Rafael M. Fernandes, Peter P. Orth, and Jörg Schmalian, "Intertwined Vestigial Order in Quantum Materials: Nematicity and Beyond," Annu. Rev. Condens. Matter Phys. **10**, 133–154 (2019).

[4] Adarsh S. Patri, Akito Sakai, SungBin Lee, Arun Paramekanti, Satoru Nakatsuji, and Yong Baek Kim, "Unveiling hidden multipolar orders with magnetostriction," Nat. Commun. **10**, 4092 (2019).

[5] Daigorou Hirai, Hajime Sagayama, Shang Gao, Hiroyuki Ohsumi, Gang Chen, Taka Hisa Arima, and Zenji Hiroi, "Detection of multipolar orders in the spin-orbit-coupled 5*d* Mott insulator Ba_2MgReO_6," Phys. Rev. Res. **2**, 022063(R) (2020).

[6] Paolo Santini, Stefano Carretta, Giuseppe Amoretti, Roberto Caciuffo, Nicola Magnani, and Gerard H. Lander, "Multipolar interactions in *f*-electron systems: The paradigm of actinide dioxides," Rev. Mod. Phys. **81**, 807–863 (2009).

[7] Gabriel Aeppli, Alexander V. Balatsky, Henrik M. Rønnow, and Nicola A. Spaldin, "Hidden, entangled and resonating order," Nat. Rev. Mater. **5**, 477–479 (2020).

[8] J.A. Mydosh and P.M. Oppeneer, "Hidden order behaviour in URu_2Si_2 (A critical review of the status of hidden order in 2014)," Phil. Mag. **94**, 3642–3662 (2014).

[9] Kristjan Haule and Gabriel Kotliar, "Arrested Kondo effect and hidden order in URu_2Si_2," Nat. Phys. **5**, 796–799 (2009).

[10] Victor Barzykin and Lev P. Gor'kov, "Singlet Magnetism in Heavy Fermions," Phys. Rev. Lett. **74**, 4301–4304 (1995).

[11] Tadao Kasuya, "Hidden Ordering and Heavy Mass in URu_2Si_2 and Its Alloys," J. Phys. Soc. Jpn. **66**, 3348–3351 (1997).

[12] Hiroaki Ikeda and Yoji Ohashi, "Theory of Unconventional Spin Density Wave: A Possible Mechanism of the Micromagnetism in U-based Heavy Fermion Compounds," Phys. Rev. Lett. **81**, 3723–3726 (1998).

[13] P. Chandra, P. Coleman, J. A. Mydosh, and V. Tripathi, "Hidden orbital order in the heavy fermion metal URu_2Si_2," Nature **417**, 831–834 (2002).

[14] V. P. Mineev and M. E. Zhitomirsky, "Interplay between spin-density wave and induced local moments in URu_2Si_2," Phys. Rev. B **72**, 014432 (2005).

[15] C. Pépin, M. R. Norman, S. Burdin, and A. Ferraz, "Modulated Spin Liquid: A New Paradigm for URu_2Si_2," Phys. Rev. Lett. **106**, 106601 (2011).

[16] R.V.K. Mangalam, Nirat Ray, Umesh V. Waghmare, A. Sundaresan, and C.N.R. Rao, "Multiferroic properties of nanocrystalline $BaTiO_3$," Solid State Commun. **149**, 1–5 (2009).

[17] Donald M. Evans, Marin Alexe, Alina Schilling, Ashok Kumar, Dilsom Sanchez, Nora Ortega, Ram S. Katiyar, James F. Scott, and J. Marty Gregg, "The Nature of Magnetoelectric Coupling in $Pb(Zr,Ti)O_3$–$Pb(Fe,Ta)O_3$," Adv. Mater. **27**, 6068–6073 (2015).

[18] Alexei A Belik, "Local distortions in multiferroic $BiMnO_3$ as a function of doping," Sci. Technol. Adv. Mater. **12**, 044610 (2011).

[19] Ling-Fang Lin, Qiao-Ru Xu, Yang Zhang, Jun-Jie Zhang, Yan-Ping Liang, and Shuai Dong, "Ferroelectric ferrimagnetic $LiFe_2F_6$: Charge-ordering-mediated magnetoelectricity," Phys. Rev. Mater. **1**, 071401 (2017).

[20] Y. Tokura and N. Nagaosa, "Orbital Physics in Transition-Metal Oxides," Science **288**, 462–468 (2000).

[21] Yoshinori Tokura and Shinichiro Seki, "Multiferroics with Spiral Spin Orders," Adv. Mater. **22**, 1554–1565 (2010).

[22] Yoshinori Tokura, Kenji Yasuda, and Atsushi Tsukazaki, "Magnetic topological insulators," Nat. Rev. Phys. **1**, 126–143 (2019).

[23] Manfred Fiebig, "Revival of the magnetoelectric effect," J. Phys. D: Appl. Phys. **38**, R123 (2005).

[24] W. Eerenstein, N. D. Mathur, and J. F. Scott, "Multiferroic and magnetoelectric materials," Nature **442**, 759–765 (2006).

[25] R. Ramesh and Nicola A. Spaldin, "Multiferroics: progress and prospects in thin films," Nat. Mater. **6**, 21–29 (2007).

[26] Sang-Wook Cheong and Maxim Mostovoy, "Multiferroics: a magnetic twist for ferroelectricity," Nat. Mater. **6**, 13–20 (2007).

[27] Daniel Khomskii, "Classifying multiferroics: Mechanisms and effects," Physics **2**, 20 (2009).

[28] Shuai Dong, Hongjun Xiang, and Elbio Dagotto, "Magnetoelectricity in multiferroics: a theoretical perspective," Natl. Sci. Rev. **6**, 629–641 (2019).

[29] Thomas Lottermoser and Dennis Meier, "A short history of multiferroics," Phys. Sci. Rev. **6**, 2020–0032 (2021).

[30] Hosho Katsura, Naoto Nagaosa, and Alexander V. Balatsky, "Spin Current and Magnetoelectric Effect in Noncollinear Magnets," Phys. Rev. Lett. **95**, 057205 (2005).

[31] Yoshinori Tokura, Shinichiro Seki, and Naoto Nagaosa, "Multiferroics of spin origin," Rep. Prog. Phys. **77**, 076501 (2014).

[32] D Bossini, D M Juraschek, R M Geilhufe, N Nagaosa, A V Balatsky, M Milanović, V V Srdić, P Šenjug, E Topić, D Barišić, M Rubčić, D Pajić, T Arima, M Savoini, S L Johnson, C S Davies, and A Kirilyuk, "Magnetoelectrics and multiferroics: theory, synthesis, characterisation, preliminary results and perspectives for all-optical manipulations," J. Phys. D: Appl. Phys. **56**, 273001 (2023).

[33] Ling-Fang Lin, Qiao-Ru Xu, Yang Zhang, Jun-Jie Zhang, Yan-Ping Liang, and Shuai Dong, "Ferroelectric ferrimagnetic $LiFe_2F_6$: Charge-ordering-mediated magnetoelectricity," Phys. Rev. Mater. **1**, 071401(R) (2017).

[34] Claude Ederer and Nicola A. Spaldin, "A new route to magnetic ferroelectrics," Nat. Mater. **3**, 849–851 (2004).

[35] L. N. Bulaevskii, C. D. Batista, M. V. Mostovoy, and D. I. Khomskii, "Electronic orbital currents and polarization in Mott insulators," Phys. Rev. B **78**, 024402 (2008).

[36] Saikat Banerjee and Shi-Zeng Lin, "Emergent orbital magnetization in Kitaev quantum magnets," SciPost Phys. **14**, 127 (2023).

[37] Saikat Banerjee, Wei Zhu, and Shi-Zeng Lin, "Electromagnetic signatures of a chiral quantum spin liquid," npj Quantum Mater. **8**, 63 (2023).

[38] William Witczak-Krempa, Gang Chen, Yong Baek Kim, and Leon Balents, "Correlated Quantum Phenomena in the Strong Spin-Orbit Regime," Ann. Rev. Condens. Matter Phys. **5**, 57–82 (2014).

[39] Tomohiro Takayama, Jiří Chaloupka, Andrew Smerald, Giniyat Khaliullin, and Hidenori Takagi, "Spin–Orbit-Entangled Electronic Phases in 4d and 5d Transition-Metal Compounds," J. Phys. Soc. Japan **90**, 062001 (2021).

[40] Gang Chen and Leon Balents, "Spin-orbit coupling in d^2 ordered double perovskites," Phys. Rev. B **84**, 094420 (2011).

[41] Giniyat Khaliullin, Derek Churchill, P. Peter Stavropoulos, and Hae-Young Kee, "Exchange interactions, Jahn-Teller coupling, and multipole orders in pseudospin one-half $5d^2$ Mott insulators," Phys. Rev. Res. **3**, 033163 (2021).

[42] Ahmed Rayyan, Derek Churchill, and Hae-Young Kee, "Field-induced Kitaev multipolar liquid in spin-orbit coupled d^2 honeycomb Mott insulators," Phys. Rev. B **107**, L020408 (2023).

[43] A. Paramekanti, D. D. Maharaj, and B. D. Gaulin, "Octupolar order in d-orbital Mott insulators," Phys. Rev. B **101**, 054439 (2020).

[44] D. D. Maharaj, G. Sala, M. B. Stone, E. Kermarrec, C. Ritter, F. Fauth, C. A. Marjerrison, J. E. Greedan, A. Paramekanti, and B. D. Gaulin, "Octupolar versus Néel Order in Cubic $5d^2$ Double Perovskites," Phys. Rev. Lett. **124**, 087206 (2020).

[45] Sreekar Voleti, D. D. Maharaj, B. D. Gaulin, Graeme Luke, and A. Paramekanti, "Multipolar magnetism in d-orbital systems: Crystal field levels, octupolar order, and orbital loop currents," Phys. Rev. B **101**, 155118 (2020).

[46] Derek Churchill and Hae-Young Kee, "Competing multipolar orders in a face-centered cubic lattice: Application to the osmium double perovskites," Phys. Rev. B **105**, 014438 (2022).

[47] Hiroaki Kusunose, "Description of Multipole in f-Electron Systems," J. Phys. Soc. Japan **77**, 064710 (2008).

[48] Leonid V. Pourovskii, Dario Fiore Mosca, and Cesare Franchini, "Ferro-octupolar Order and Low-Energy Excitations in d^2 Double Perovskites of Osmium," Phys. Rev. Lett. **127**, 237201 (2021).

[49] Satoru Hayami and Hiroaki Kusunose, "Microscopic Description of Electric and Magnetic Toroidal Multipoles in Hybrid Orbitals," J. Phys. Soc. Jpn. **87**, 033709 (2018).

[50] See the Supplementary Material for more details.

[51] Giniyat Khaliullin, "Excitonic Magnetism in Van Vleck–type d^4 Mott Insulators," Phys. Rev. Lett. **111**, 197201 (2013).

[52] Christopher Svoboda, Mohit Randeria, and Nandini Trivedi, "Effective magnetic interactions in spin-orbit coupled d^4 Mott insulators," Phys. Rev. B **95**, 014409 (2017).

[53] Antoine Georges, Luca de' Medici, and Jernej Mravlje, "Strong Correlations from Hund's Coupling," Annu. Rev. Condens. Matter Phys. **4**, 137–178 (2013).

[54] Umesh Kumar, Saikat Banerjee, and Shi-Zeng Lin, "Floquet engineering of Kitaev quantum magnets," Commun. Phys. **5**, 157 (2022).

[55] P Hoffmann, "Generalization of Stevens' operator-equivalent method," J. Phys. A: Math. Gen. **24**, 35 (1991).

[56] SangEun Han, Daniel J. Schultz, and Yong Baek Kim, "Non-Fermi liquid behavior and quantum criticality in cubic heavy fermion systems with non-Kramers multipolar local moments," Phys. Rev. B **106**, 155155 (2022).

[57] O. Nganba Meetei, Onur Erten, Mohit Randeria, Nandini Trivedi, and Patrick Woodward, "Theory of High T_c Ferrimagnetism in a Multiorbital Mott Insulator," Phys. Rev. Lett. **110**, 087203 (2013).

[58] Kliment I Kugel' and D I Khomskiĭ, "The Jahn-Teller effect and magnetism: transition metal compounds," Sov. Phys. Usp. **25**, 231 (1982).

[59] A. Abragam and B. Bleaney, *Electron Paramagnetic Resonance of Transition Ions*, International series of monographs on physics (Clarendon P., 1970).

[60] Giniyat Khaliullin, "Orbital Order and Fluctuations in Mott Insulators," Prog. Theor. Phys. Suppl. **160**, 155–202 (2005).

[61] Adrien Bolens, "Theory of electronic magnetoelectric coupling in d^5 Mott insulators," Phys. Rev. B **98**, 125135 (2018).

[62] J. C. Slater and G. F. Koster, "Simplified LCAO Method for the Periodic Potential Problem," Phys. Rev. **94**, 1498–1524 (1954).

[63] J. R. Schrieffer and P. A. Wolff, "Relation between the Anderson and Kondo Hamiltonians," Phys. Rev. **149**, 491–492 (1966).

[64] A. Brooks Harris and Robert V. Lange, "Single-Particle Excitations in Narrow Energy Bands," Phys. Rev. **157**, 295–314 (1967).

[65] Sreekar Voleti, Arijit Haldar, and Arun Paramekanti, "Octupolar order and ising quantum criticality tuned by strain and dimensionality: Application to d-orbital mott insulators," Phys. Rev. B **104**, 174431 (2021).

[66] Diptiman Sen and R. Chitra, "Large-U limit of a Hubbard model in a magnetic field: Chiral spin interactions and paramagnetism," Phys. Rev. B **51**, 1922–1925 (1995).

[67] Nicholas Metropolis, Arianna W. Rosenbluth, Marshall N. Rosenbluth, Augusta H. Teller, and Edward Teller, "Equation of State Calculations by Fast Computing Machines," J. Chem. Phys. **21**, 1087–1092 (1953).

[68] Koji Hukushima and Koji Nemoto, "Exchange Monte Carlo Method and Application to Spin Glass Simulations," J. Phys. Soc. Jpn. **65**, 1604–1608 (1996).

[69] K. F. Mucker, G. S. Smith, and Q. Johnson, "The crystal structure of $ReCl_5$," Acta Crystallogr. B **24**, 874–879 (1968).

[70] M. M. Korshunov, I. A. Nekrasov, N. S. Pavlov, and A. A. Slobodchikov, "Band Structure of Tungsten Oxide W_20O_58 with Ideal Octahedra," JETP Lett. **113**, 57–60 (2021).

[71] David C. Palmer, "Visualization and analysis of crystal structures using CrystalMaker software," Z. Kristallogr. Cryst. Mater. **230**, 559–572 (2015).

[72] Sang-Wook Cheong and Fei-Ting Huang, "Altermagnetism with non-collinear spins," npj Quantum Mater. **9**, 13 (2024).

[73] Sang-Wook Cheong and Fei-Ting Huang, "Kinetomagnetism of chirality and its applications," Appl. Phys. Lett. **125**, 060501 (2024).

[74] Aria Mansouri Tehrani, Jian-Rui Soh, Jana Pásztorová, Maximilian E. Merkel, Ivica Živković, Henrik M. Rønnow, and Nicola A. Spaldin, "Charge multipole correlations and order in Cs_2TaCl_6," Phys. Rev. Res. **5**, L012010 (2023).

[75] Denis Golež, Martin Eckstein, and Philipp Werner, "Multiband nonequilibrium GW+EDMFT formalism for correlated insulators," Phys. Rev. B **100**, 235117 (2019).

[76] Pengwei Zhao, Jiahao Yang, and Gang v. Chen, "Multipolar Ferroelectricity in the Mott Regime," (2024), arXiv:2412.18942.